# Harnessing the hERG1/β1 integrin complex via a novel bispecific single-chain antibody: an effective strategy against solid cancers

Claudia Duranti[1], Jessica Iorio[1], Tiziano Lottini[1], Elena Lastraioli[1], Silvia Crescioli[1*], Giacomo Bagni[1], Matteo Lulli[2], Chiara Capitani[1#], Rayhana Bouazzi[1#], Matteo Stefanini[3], Laura Carraresi[3], Luisa Iamele[4], Hugo De Jonge[4], and Annarosa Arcangeli[1,5§]

[1] Department of Experimental and Clinical Medicine, Section of Internal Medicine, University of Florence, Viale GB Morgagni 50, 50134 Firenze, Italy

[2] Department of Biomedical and Clinical Sciences, Section of General Pathology, University of Florence, Viale GB Morgagni 50, 50134 Firenze, Italy

[3] Dival Toscana S.r.l., Via Madonna del Piano 6, 50129 Sesto Fiorentino (FI), Italy

[4] Department of Molecular Medicine, University of Pavia, via Ferrata 9, 27100 Pavia, Italy

[5] CSDC-Center for the Study of Complex Dynamics, via Sansone, 1, 50019 Sesto Fiorentino, Florence, Italy

*Present address St John`s Institute of Dermatology, School of Basic and Medical Biosciences, King`s College London, London, UK.

# Department of Medical Biotechnologies, University of Siena, Strada delle Scotte, 4

53100 , Siena, Italy.

§ corresponding author:

Prof. Annarosa Arcangeli
Department of Experimental and Clinical Medicine, Section of Internal Medicine, University of Florence
Viale GB Morgagni 50, 50134 Firenze, Italy.
Telephone: +39 055 2751285
Fax: +39 055 2751281
Email: annarosa.arcangeli@unifi.it

**Running title**: diabodies targeting the hERG1/β1 molecular complex

**Keywords**: bispecific antibodies, single-chain diabody, hERG1 potassium channels, integrins, photoacustic cancer imaging , preclinical characterization

**ABSTRACT:**

Monoclonal antibodies (mAbs), either mono- or bispecific (bsAb), represent one of the most successful approaches to treat many types of malignancies. However, there are certain limitations to the use of full length mAbs for clinical applications, which can be overcome by engineered antibody fragments. The aim of the present study was to develop a small bsAb, in the format of a single-chain diabody (scDb), to efficiently target two proteins, the hERG1 potassium channel and the β1 subunit of integrin receptors, which specifically form a macromolecular complex in cancer cells.

We provide evidence that the scDb we produced binds to the hERG1/β1 complex in cancer cells and tissues, whereas does not bind to the hERG1 channel in non-pathological tissues, in particular the heart. The scDb-hERG1-β1 (1) downregulates the formation of the hERG1/β1 complex, (2) inhibits Akt phosphorylation and HIF-1α expression and (3) decreases cell survival, proliferation and migration *in vitro*. These effects only occur in cancer cells (either colon, pancreatic or breast), but not in normal cells. *In vivo*, the scDb-hERG1-β1 shows a good pharmacokinetic profile, with a half-life of 13.5 hours and no general, cardiac or renal toxicity when injected intravenously up to the dose of 8 mg/Kg. The scDb-hERG1-β1 accumulates into subcutaneous xenografted tumors, arising from either colon or pancreatic human cancer cells, and induces a reduction of tumor growth and vascularization.

Overall, the scDb-hERG1-β1 represents an innovative single-chain bispecific antibody for therapeutic applications in solid cancers which over express the hERG1/β1 integrin signaling complex.

## INTRODUCTION

Over the past twenty years, therapeutic antibodies have rapidly become the leading product within the biopharmaceutical market (1,2). Particularly relevant has been the development of bispecific antibodies (bsAbs), which nowadays represent a breakthrough in cancer immunotherapy (3,4). First, by combining a tumor-targeting binding site with one that binds to specific immune cells, bsAbs present enhanced tumor killing capability (5). Second, by interacting with two different cell-surface antigens, bsAbs can simultaneously modulate two different signaling pathways (6), or increase the binding specificity to cancer cells, thus improving the efficacy and specificity of antibody drug conjugates (ADC) (7). Indeed, more than 30 bsAbs are actually in clinical development (8). However, treating solid tumors with full length antibodies is hampered by their inefficient delivery to tumors, mainly because of the properties of the immunoglobulin molecule itself. This results in both heterogeneous distribution inside tumors and body, and possible occurrence of systemic toxic effects (9). Such issues have been addressed by developing much smaller antibody fragments, which overall have an increased vascular permeability, and diffuse more rapidly into tumors (10).

Current effort is directed at developing novel bsAbs formats, which better penetrate into cancer tissues, and more efficiently recognize their target(s) and modulate appropriate signaling pathways. In this scenario, either established or novel tumor specific antigens are employed (11).

We have recently discovered a novel oncological target: the complex between the potassium channel encoded by the *ether-à-go-go–related gene 1* (hERG1) and the β1 subunit of integrin adhesion receptors (β1 integrin) (12-14). hERG1 is physiologically expressed in human cardiomyocytes, where it represents the molecular correlate of the repolarizing current IKr (15), and in other excitable cells, such as neurons and insulin-secreting pancreatic beta cells (16). Furthermore, hERG1 is mis- and over-expressed in several types of human cancers (reviewed in 17). In tumors, hERG1 resides in a peculiar conformational state, strictly bound to the β1 integrin, within a macromolecular complex where the two proteins are at a distance less than 1 nm (14). This

does not occur in the heart, where hERG1 is bound to classical accessory subunits, such as the *potassium voltage-gated channel subfamily E regulatory subunit 1* KCNE1 (14). In cancer cells, the hERG1/β1 integrin complex is triggered by integrin-mediated adhesion to proteins of the extracellular matrix (12,13,18) which leads to the activation of intracellular signaling pathways, mainly centered on PI3K and Akt (19). These signaling pathways in turn control cancer cell survival, proliferation and migration, and promote tumor progression and metastatic spread (20). Hence, the hERG1/β1 complex represents a tumor-specific antigen (14,20), whose therapeutic targeting would produce favorable antineoplastic effects while avoiding the occurrence of the typical cardiac side effects produced by hERG1 current's blockers (21, 22).

To investigate this possibility, we designed a bispecific antibody in the format of a single-chain Diabody (scDb). Diabodies are a peculiar class of bsAbs, being small antibody fragments with two antigen-binding sites which reside in a bivalent scFv dimer (23, 24). Because of their small size, scDbs can penetrate into cancer tissues, and simultaneously bind to the hERG1/β1 integrin complex on the plasma membrane of cancer cells, hopefully harnessing the complex and its downstream signaling effects.

We provide here evidence that the scDb-hERG1-β1 efficiently binds to the hERG1/β1 integrin complex in cancer cells, whereas does not bind to the hERG1 channel in the heart. In this way, the scDb-hERG1-β1 exerts significant anti-neoplastic activity, both *in vitro* and *in vivo*. Our results indicate a potential anti-cancer approach for those cancers which over-express the hERG1/β1 integrin complex.

## MATERIALS AND METHODS

### Cell Culture

HEK293, PANC-1, MIA PaCa2 and HCT116 cells were obtained from the American Type Culture Collection (ATCC); MDA-MB-231 were a kind gift of Prof. M.B.Djamgoz (Department of Life Sciences, Imperial College, London); SH-SY5Y and GD25 cells were a kind gift of Prof. P. Defilippi (Department of Molecular Biotechnology and Health Sciences, University of Turin, Italy). Cells were routinely cultured at 37 °C with 5% $CO_2$ in a humidified atmosphere, in RPMI (Euroclone) (HCT116, SH-SY5Y cells) or in Dulbecco's modified Eagle's Medium (DMEM; Euroclone) (HEK293 PANC1, MIA PaCa-2 and MDA-MB-231), supplemented with 2% L-Glut and 10% (5% for MDA-MB-231 cells) fetal bovine serum (FBS, Fetal Bovine Serum EU Approved, Euroclone, Pero, Italy). We certify that all the cell lines used in the present study were routinely screened for Mycoplasma contamination, and only Mycoplasma negative cells were used. HEK293 cells and MDA-MB-231 cells expressing the hERG1 construct were prepared as previously described (14), and maintained in complete culture medium supplemented with either 0.8 mg/ml (for HEK293 cells) or 2.0 mg/ml (for MDA-MB-231 cells) of Geneticin (G418, Thermo Fisher Scientific, Waltham, MA). Transient transfection of GD25 cells with hERG1 was performed as in [14].

For treatment with the scDb, cells were harvested from a semiconfluent culture, detached with 5 mM EDTA in PBS (PBS-EDTA), and seeded in complete medium at the following concentrations: $1x10^3$ cells/well in 96 wells plates for spheroids' formation; $7.5 \times 10^3$ cells/well in 96 wells plates for cell ELISA and cell proliferation assay; $1 \times 10^4$ cells/well in 96 wells plates for viability assay; $5x10^5$ per dish in 35 mm Petri dishes for migration assay, immunofluorescence and protein extraction. In any case, cells were incubated for different times in control conditions (medium plus

the vehicle) or in medium containing the scDb at different concentrations. In particular, for **cell viability assay**, cells were treated with 0, 5, 10, 20, 50, 100 μg/ml scDb for 24 hours, then detached with PBS-EDTA and counted with Trypan Blue (Thermo Fisher Scientific). $IC_{50}$ values were determined as in (19) using the Origin Software (OriginLab Corporation, Northampton, MA). **Cell proliferation** was determined as in (19), by determining the number of vital cells, and adding the scDb at the $IC_{50}$ determined for each cell line. For **spheroid formation assay,** PANC-1, MIA PaCa-2 and HCT-116 cells were seeded on an agarose base layer (1.5 g/l) in 96 wells plates and grown for 72 hours. Then the scDb was added at the $IC_{50}$ concentration determined for each cell line, as above. Spheroid growth was monitored taking photos every 24 hours using a Nikon Eclipse TE300 microscope, and analyzing their volume using Spheroid Sizer software (MathLab Inc). **Lateral motility** was assessed by a monolayer wound assay as described in (18), adding the scDb either at the $IC_{50}$ concentration determined for each cell line, or at 50 or 100 μg/ml.

**Enzyme-Linked Immunosorbent Assay (ELISA)**

*Peptide ELISA***.** The following peptides were used: S5-P hERG1 peptide (sequence: EQPHMDSRIGWLHN) (25) and β1-TS2/16 peptide (sequence: NKGEVFNELVGK) (26) (Eurofins, Luxembourg). Peptides were diluted in 1mM $Na_2CO_3$ at pH 9.6 at 10 μg/ml final concentration and used, either separately or mixed at a 1:1 ratio (5 μg+ 5 μg/ml), to coat a 96 wells plate. The procedure was as described in (27), employing the anti-6xHis antibody followed by anti-mouse IgG-HRP conjugate (see Supplementary Materials). EC50 was determined either using Prism or accoding to what reported in https://recombinant-antibodies.org i.e. by inspection to determine the OD at which saturation occurs, dividing by 2 and interpolating the concentration of rAB that results in this absorbance. The ELISA assay was also used to determine scDb binding to cells (Cell-ELISA) as in (28), serum stability and *in vivo* half-life (see Supplementary Methods).

**Immunofluorescence (IF)**

IF on cells was performed following the protocol previously described in (27). For IF on cardiac tissue, fresh human tissue from healthy atrium was obtained by the Department of Cardiac Surgery

of the Azienda Ospedaliero-Universitaria Senese, snap frozen in liquid nitrogen and cut with a cryostat in 5µm sections. After 2 hours of blocking in PBS with 10% BSA, sections were incubated for further 2 hours with either scDb-hERG1-β1 or scFv hERG1 antibodies (20 µg/ml and 200 µg/ml final concentrations), followed by 1 hour with anti-6xHis (Abcam, Cambridge, UK) and then 1 hour with anti-mouse Alexa Fluor 488 (Thermo Fisher Scientific, Waltham, MA). Incubation with mAb hERG1 was performed O/N at a final concentration of 1 µg/ml. All incubations were performed at room temperature. Nuclei were stained with Hoechst (1:1000 in PBS, 45 minutes; Merck Sigma, Burlington, MA). Images were captured using confocal microscope, Nikon TE2000.

**Animal studies**

All the *in vivo* experiments were performed at the Animal Facility of the University of Florence (CESAL). Mice were housed in filter-top cages with a 12-hour dark-light cycle and had unlimited access to food and water. All the procedures were approved by the Italian Ministry of Health (369/2018-PR and 182/2019-PR).

*Pharmacokinetics*

Athymic Nude-Foxn1nu (nu/nu) (Envigo) mice were injected with 160 µg (8 mg/Kg) of scFv-hERG1-Cys antibody and blood samples were collected from the tail vein at 0, 5, 15, 30, 120, 360, 1440, 2880 minutes after antibody injection. Each sample was spun at 12000 rpm for 5 minutes and the resulting plasma was stored at −80° C until analyzed. The plasma concentration of scFv-hERG1-Cys antibody was determined by sandwich ELISA (see Materials and Methods in the main text), using anti -6xHis antibody (Abcam, Cambridge, UK) 1:250 in PBS + 3% BSA to reveal the scDb-hERG1-β1, followed by anti-mouse IgG-HRP conjugate (Merck Sigma, Burlington, MA) 1:500 in PBS + 3% BSA, as described in (24).The half-lives for elimination phase were determined using Origin 7.0 Software by fitting the last four data points into the first-order equation, $T1/2 = (\Delta t/t1\text{-}t0)/\Delta C$ where $(\Delta t/t1\text{-} t0)$ represents the slope of the curve and $\Delta C$ represents the value corresponding to the half of the antibody concentration at t1, which corresponds to T=0. The serum stability against proteolytic activities of the scDb-hERG1-β1 was assessed using 20 µg of antibody.

The scDb was incubated at 37°C in mouse serum up to 96 hours (0, 6, 24, 48, 72, 96 hrs) and its concentration was determined through a sandwich ELISA assay.

*Xenografts*

Female Nude-Foxn1nu (nu/nu) mice (Envigo) aged 6 weeks were injected subcutaneously (s.c) in either flanks with $1x10^{6}$ cells previously resuspended in 100µl of PBS. Two xenograft mouse model were performed: one PDAC, by the injection of PANC-1 and one CRC by the injection of HCT-116. Each xenograft mouse model was divided in two group of treatment: one group of mice was treated with saline solution and one group was treated with 8 mg/kg of scDb-hERG1-β1. Mice inoculated with HCT 116 were i.v. administered with scDb-hERG1-β1 antibody with six single doses after 5 days from the injection. Mice inoculated with PANC-1 were i.v. administered with scDb-hERG1-β1 antibody with eleven doses after 11 days from the injection.

*Ultrasound (US) imaging*

3D micro-ultrasound echography was performed on live animals before the first treatment and once a week until the experimental end point, by using VevoLAZR-X system (Visualsoncs Fujifilm). The volumes were measured delineating the ROI (Region Of Interest) for each axial slide using the Vevo LAB software. B-Mode imaging were performed with the Vevo LAZR-X 55-MHz transducer. Mice were anesthetized by 1,5/2% isoflurane and placed on a pad heated at 37°C and ECG, body temperature and respiration were monitored for the duration of acquisition and the respiratory gating was derived from ECG.

Kidneys perfusion status were assessed by using 2D Non Linear Contrast mode (NLC) imaging by the i.v. injection of a 50µl bolus Vevo MicroMarkers (Bracco Research s.p.a.) as contrast agents (corresponding to $2 \times 10^{7}$ bubbles/50µl bolus), by using 27G butterfly syringe. Fresh dilution of the stock contrast agent should be completed just prior to each injection. The mouse was positioned on prone position on the table for imaging. The first acquisition was performed in B-mode to

visualize both kidneys in the same frame. 21-MHz transducer was used for the NLC imaging. Data obtained were processed with the VevoCQ (Fujifilm Visualsonics).

**Human samples collection**

Archival paraffin embedded samples of colorectal, breast and pancreatic cancer were retrieved and collected by different institutions in Italy after informed written consent. In particular, colorectal cancers were obtained by the Section of Pathological Anatomy of the following insitutions: Department of Experimental and Clinical Medicine of the University of Florence, Campus Bio-Medico University of Rome and Spedali Civili Hospital, Brescia. All breast cancer samples were obtained by the Section of Pathological Anatomy, Department of Surgery and Translational Medicine, University of Florence - Azienda Ospedaliero-Universitaria Careggi, Florence. Pancreatic cancer samples were obtained from Department of Experimental and Clinical Medicine of the University of Florence, Campus Bio-Medico University of Rome. Normal heart atrium paraffin embedded slides were purchased from D.B.A. Italia.

In order to perform IF experiments, fresh human heart tissue from healthy atrium were obtained by the Department of Cardiac Surgery of the Azienda Ospedaliero-Universitaria Senese, snap frozen in liquid nitrogen and then cut with a cryostat in 5⌈m sections. Details of the IF protocol are in the Materials and Methods section of the main text.

**Antibodies, Reagents, Production of the Diabody targeting hERG1 and the β1 integrin (scDb-hERG1-β1), Induction of large scale scDb-hERG1-β1 protein expression, Immunohistochemistry and Statistical Analysis.**

Please see Supplementary data for this article.

## RESULTS

### *Generation of a single-chain diabody (scDb) targeting the hERG1/β1 complex (scDb-hERG1-β1)*

The scDb-hERG1-β1 was developed starting from two single chain Fragment variable (scFv) antibodies, one directed against hERG1 (scFv-hERG1from mAb-hERG1) (27) and one against the β1 integrin (scFv-β1 from mAb-β1 TS2/16). The VH and VL sequences of the two scFv(s) were joined by three peptide linkers (A, M and B), in the following order: $VH_{hERG1}$- linker A-$VL_{β1}$-linker M-$VH_{β1}$-linker B-$VL_{hERG1}$ (Figure 1A). Linker M was 20 amino acid long, to allow the proper assembly of the protein in a Diabody format (23). The $VH_{hERG1}$ sequence was mutagenized substituting a Phe with a Cys amino acid in residue 92 (highlighted in red in Figure 1B), to improve scDb-hERG1-β1 stability and specificity (27). Details of scDb-hERG1-β1 development are in Supplementary Methods and Tables S1 and S2. The deduced amino acid sequence of the scDb-hERG1-β1 is in Figure 1B.

The scDb-hERG1-β1 in pPIC9K vector was used to transform yeast cells from the GS115 *Pichia pastoris* strain. Colonies capable of growing in the presence of the selection antibiotic Geneticin were chosen, grown in a small volume liquid culture and screened for protein secretion by dot blot. Sixty-seven colonies were screened, and those with the highest signal were used for large scale production, affinity chromatography purification and further characterization by Coomassie blue staining and Western Blot (WB). Representative data of the scDb-hERG1-β1 secreted by two of the best colonies (either 3G5 or 3G9) are shown in Figure 1C-E. The chromatogram obtained by affinity chromatography shows a peak consistent with the elution of a single protein (Figure 1C). Coomassie Blue staining (Figure 1D) and WB (Figure 1E) show a single band of 68 kDa. Data from other screened colonies are in Figure S1A and S1B. Both 3G5 and 3G9 colonies produced the scDb-hERG1-β1 at a mean yield of 2.3 mg per liter of yeast culture, which was stable at +4°C for at least 10 weeks (Figure S1B).

### *The scDb-hERG1-β1 efficiently binds to the hERG1/β1 integrin in complex.*

The binding of the scDb-hERG1-β1 to its antigen(s) was first assessed by ELISA, using the two peptides recognized by the original monoclonal antibodies. Peptides were used either separately or mixed at a 1:1 ratio. The scDb-hERG1/β1 bound with high affinity and a clear dose-dependence to the mix of the two peptides (Figure 1F), with an $EC_{50}$ of 21.3 μg/ml, while only slightly bound to the single peptides (Figure 1G). The two mAbs used as templates for scDb development bound to their corresponding peptides, and not to the unrelated peptide or the two mixed peptides (Figure S2A and S2B). Only the anti-hERG1 mAb bound to the mixed peptides, although at much lower affinity compared to the scDb (Figure S2A).

These data suggest that the scDb-hERG1-β1 recognizes the two proteins, hERG1 and β1 integrin, once complexed in live cells. To confirm this, we performed a cell–ELISA on cells with variable expression of the complex (14): GD25 cells (normal cells knock out for the β1 integrin (14)); GD 25-hERG1-T (GD25 cells transiently transfected with hERG1, hence expressing only the hERG1 channel); HEK 293 cells (normal cells with β1 integrin expression but no hERG1); HEK 293-hERG1-T (hERG1-transfected HEK cells with a significant expression of the hERG1/β1 complex); MDA-MB-231 cells (Breast Cancer (BCa) cells with low expression of the complex); MDA-MB-231-hERG1-T (hERG1 transfected BCa cells with high expression of the complex); SH-SY5Y neuroblastoma cells (12), HCT116 Colon Cancer (CC) cells (13), PANC-1 and MIAPaCa2 Pancreatic Ductal Adeno Carcinoma (PDAC) cells (29,30), all with high expression of the hERG1/β1 complex. When used at concentrations ranging from 5 to 40 μg/ml, the scDb-hERG1-β1 bound to living cells with an intensity that depended on both the dose of the scDb and the amount of the expressed hERG1-β1 complex (Figure 1H). A crude supernatant from a negative yeast colony showed no binding (Figure S3).

Indirect IF was then performed on some of the cell lines listed above. MDA-MB-231-hERG1-T, HCT116 and PANC-1 showed a clear signal, mainly at the plasma membrane level. On the contrary, MDA-MB-231 cells had a low signal and HEK 293 cells were completely negative (Figure 2A).

The scDb-hERG1-β1 was then tested on both normal human heart, where hERG1 is highly expressed but not complexed to the β1 integrin (14), and cancer tissues where hERG1 is over-expressed (31) and forms a complex with the β1 integrin (14). The scDb did not show any staining, either IF or IHC, in human cardiac myocytes, even when its concentration was increased from 20 to 200 μg/ml (Figure 2B and 2C, panels on the left). On the contrary, both the scFv-hERG1 and the hERG1-mAb gave a strong staining (Figure 2B and 2C, middle and right panels). The scDb-hERG1-β1 gave a good IHC signal on different human cancers: CC, PDAC and BCa (Figure 2D). Notably, the scDb did not show any immunoreactivity on a normal pancreatic insula, sometimes visible in PDAC samples, which contains insulin secreting beta cells which are known to express hERG1 currents (32) (panel "Normal pancreas" in Figure 2D). For comparison, a pancreatic insula labelled with the mAb-hERG1 is reported in the inset: a positive signal ascribable to a hERG1-positive insulin secretin cell (see the arrow) is evident, confirming what shown in [29].

Overall, the scDb-hERG1-β1 only binds to the hERG1/β1 complex in cancer cells and tissues, while spares the hERG1 channel not complexed to the integrin.

***The scDb-hERG1-β1 impairs the signaling pathways downstream to the hERG1/β1 integrin complex and reduces cell proliferation and migration of cancer cells.***

We then analyzed whether the scDb affected either the formation of the hERG1/β1 integrin complex, or its downstream Akt-centered signaling pathways (14,19,20). To this purpose, HCT116 CC cells or PANC-1 PDAC cells were treated over night with 100 μg/ml of scDb, and the formation of the hERG1/β1 complex (witnessed by the co-immunoprecipitation of the two proteins), Akt phosphorylation and HIF-1α expression were determined. The scDb-hERG1-β1 significantly decreased the formation of the hERG1/β1 integrin complex, as well as Akt

phosphorylation and HIF-1α expression, both in HCT116 (Figure 3A) and in PANC-1 cells (Figure 3B).

These results prompted us to test the effects of the scDb-hERG1-β1 on cell vitality, proliferation and motility. The scDb-hERG1-β1 decreased the vitality of those cancer cells with a significant hERG1/β1 complex expression, while had no effect ($IC_{50}$ > 200 μg/ml) on normal HEK 293 cells. $IC_{50}$ values determined after 24 hours of treatment are in Figure 3C and the dose-dependence curves are in Figure S4. The effect on cell vitality was stronger when the dose of the scDb-hERG1-β1 was increased up to 100 μg/ml (Figure 3D). When used at the same dose, the mAb hERG1 caused a small decrease in cell vitality, while the mAb β1 TS2/16 had no effects (Figure 3D). The scDb-hERG1-β1, used at the $IC_{50}$ dose, significantly decreased the proliferation rate of both HCT116 and PANC-1 cells (Figure 3E,G). At 96 hours of treatment, a significant percentage of dead cells was detected in HCT116 cells treated with the scDb-hERG1-β1 (Figure 3E, panel on the right). This effect was mirrored by a high number of cells in apoptosis, with no effects on the cell cycle phases (Figure 3F). In PANC-1 cells, the scDb-hERG1-β1 slowed down cell proliferation, with only a slight increase of the percentage of dead cells at 96h of treatment, compared to untreated cells (CTR) (Figure 3G, panel on the right). This effect was accompanied by an increase of cells in G1 and a decrease of cells in G2-M (Figure 3H), with almost no effects on apoptosis (Figure 3H). A similar effect was observed in MIA PaCa2 PDAC cells (Figure S5A).

The scDb-hERG1-β1 was then tested on cells cultured in 3D as spheroids, adding it after 72 hours of seeding (indicated as T=0 in Figure 4 A-C), when spheroids start to grow. When used at the $IC_{50}$ dose determined for each cell line in 2D cultures, the scDb-hERG1-β1 significantly reduced the growth rate of HCT116 and PANC-1 cancer cells, while had almost no effect on normal HEK 293 cells (Figure 4A). Data relative to MIA PaCa2 and MDA-MB-231 are in Figure S6A. No effects were observed on HCT116 cells with either the mAb hERG1 or the mAb β1 TS2/16 (Figure 4B, data relative to PANC-1 and MIA PaCa2 cells are in Figure S6B). The scDb-hERG1-β1 induced a

stronger reduction of HCT116 spheroids' growth, when it was added either at a higher concentration (100 μg/ml) or daily at the $IC_{50}$ dose (Figure 4C). The pictures of all the spheroids are in Figure S7 A-C.

Finally, the scDb-hERG1-β1 significantly reduced the motility index (MI) of those cancer cells with a significant expression of the hERG1/β1 complex, while did not affect the MI of normal HEK 293 cells (Figure 4D). This effect was stronger with a higher dose (50 μg/ml) of the scDb (Figure 4E), while null with either the mAb hERG1 or the mAb β1 TS2/16 (Figure 4F).

Overall, the scDb-hERG1-β1 shows a good antiproliferative and antimigratory activity *in vitro*.

***The scDb-hERG1-β1 shows a good pharmacokinetic profile and no (cardiac and renal) toxicity in vivo.***

Before analyzing whether the scDb-hERG1-β1 had any activity in mice *in vivo,* we determined whether it was stable against proteolytic activities contained in serum. Roughly 80% of the original scDb-hERG1-β1 was still present after 96 hours of incubation at 37°C in mouse serum (Figure 5A), indicating that it is relatively stable in serum.

The scDb-hERG1-β1 was then injected intravenously (i.v.) at 160 μg/ mouse, i.e. 8 mg/Kg,a dose compatible with that used in (33), into immunodeficient athymic Nude-Foxn1nu (nu/nu) mice and its plasma concentrations were determined by ELISA at different time points. A characteristic two-phase PK behavior emerged, with a rapid distribution phase and a longer elimination phase (Figure 5B). The half-life of the elimination phase turned out to be 13.5 hours. Before moving further to *in vivo* studies, we assessed the high (> 92%) homology of the two antigens (hERG1 and the β1 integrin, respectively) recognized by the scDb-hERG1-β1 in humans and mice ( Figure S8). The accumulation of the scDb-hERG1-β1 in internal organs (heart, liver and kidney) was determined by IHC, 3h after its injection at 8 mg/Kg. The diabody did not accumulate in the heart (Figure 5C),

confirming what occurs in fixed human hearts . Consistently, no alterations in the ECG were observed, in particular no lengthening of the QT interval (Figure 5D). The scDb-hERG1-β1 slightly accumulated in the liver and in the kidneys, in the glomerular area (Figure 5C). This finding was expected, as the molecular weight of diabodies does not allow them to freely pass the renal threshold. To assess whether such renal accumulation somehow affected renal functions, we determined the perfusion index (PI) of the kidneys in mice treated with the scDb-hERG1-β1. Ultrasound imaging in non-linear contrast mode, after microbubble injection (34), was applied (Video S1 A-D). The PI slightly decreased 3 hours after scDb-hERG1-β1 injection, recovered at 24 hours, and fully restored after 48 hours (Figure 5E). Consistently, no histological signs of renal damage were observed (Figure 5F). Finally, no signs of general toxicity (i.e. abnormal posture, back-arching, reduced mobility) or death were observed in mice after eleven, either daily or every two days (see below) injections of 8 mg/kg of scDb-hERG1-β1.

***The scDb-hERG1-β1 accumulates into tumor xenografts, reduces tumor growth and perfusion, and decreases pAkt and HIF-1α.***

The effects of the scDb-hERG1-β1 were then tested on subcutaneous (s.c.) xenografts cancer models, obtained by injecting either HCT116 human CC or PANC-1 human PDAC cells into nu/nu mice. The scDb-hERG1-β1 was administered i.v. at 8 mg/Kg, following the two different schedules shown in Figure 6A and 6F (i.e. administration of the scDb daily for 7 days for HCT 116 xenografted mice and every other day for 21 days for PANC-1 xenografted mice). The volume of the tumor masses, their oxygenation and perfusion were monitored by high resolution ultrasound (US) 3D imaging. The treatment was discontinued at day 11 for the CC model, or at day 33 for the PDAC model, mice were sacrificed and the excised tumor masses were processed for IHC analysis. The scDb-hERG1-β1 accumulated into tumor masses, either CC (Figure 6B) or PDAC (Figure 6G), and significantly slowed down tumor growth, as witnessed by the decreased tumor volume at day 11 for CC (Figure 6C and D) and at day 33 for PDAC (Figure 6H and I). In the CRC model the oxygenation status of the tumor masses was monitored in live animals by Photoacoustic (PA)

imaging. A different pattern of oxygenation, with an inner hypoxic area, was observed in the tumor masses at the end of treatment with the scDb-hERG1-β1 compared to controls (Figure 6D; contrast-enhanced ultrasound imaging videos are in Video S2 A, B). All these effects were accompanied by a significant decrease of both pAkt and HIF-1α staining (Figure 6E and J).

Overall, the scDb-hERG1-β1 shows good antineoplastic efficacy *in vivo*.

**DISCUSSION**

In the present paper we describe the development of a novel bsAb, in the format of a single-chain Diabody (scDb), which dually targets two proteins, the hERG1 potassium channel and the β1 subunit of integrin receptors, which specifically form a macromolecular signaling complex on the plasma membrane of cancer cells (14). The diabody bound with high affinity to the two proteins only when they are linked together, as occurs in cancer cells, while spared normal cells, which do not express hERG1, or the heart where hERG1 is expressed but not complexed with the integrin. The scDb-hERG1-β1 exerted antiproliferative (either inducing apoptosis or modulating the cell cycle phases) and anti-migratory effects only on cancer cells. These effects can be traced back to an inhibition of the signaling activities (impacting on AKT and HIF-1α) of the hERG1/β1 integrin complex. Furthermore, once injected *in vivo* in mice, the scDb-hERG1-β1 showed a good pharmacokinetic and toxicologic profile, accumulated into xenografted tumor masses, reducing their volume and vascularization.

The scDb-hERG1-β1 was developed through a novel procedure, starting from two different scFv antibodies, the scFv-hERG1 in the VH-VL and the scFvβ1 in the VL-VH order, and cloning the scFv β1 in the middle of the linker sequence, between $VH_{hERG1}$ and $VL_{hERG1}$. This led to balance the length of the linkers, which allowed the proper final assembly in the diabody. The construct was mutagenized in the $VH_{hERG1}$, substituting a Phe with a Cys amino-acid, to improve its performances and stability (27,35), and was expressed in yeasts, which allow proper protein glycosylation and easy production of secreted proteins (36). Indeed, the scDb-hERG1-β1 was produced in large amounts, was stable at 4°C, and showed a good binding to its dual target, whilst almost did not bind to the single peptides. The scDb-hERG1-β1 showed also a good binding to live cells, which did not saturate at 40 μg/ml, a feature which allowed us to increase its concentration in functional assays.

We chose the format of a single-chain diabody because of its small size, which ensures a good penetration into cancer tissues (24), that often present several hindrances for the efficient delivery

and homogeneous distribution of full length antibodies (37). Indeed, the scDb-hERG1-β1 well accumulated into tumor masses once injected i.v.. This was also attributable to its favorable half-life, i.e. 13.5 hours. Indeed, antibody fragments usually suffer a short serum half-life (from 10-30 min of scFvs to 3-4 hours of Fab fragments (10,37)), which may ultimately impair them to reach and to be retained in the tumor (9,38). On the contrary, the scDb-hERG1-β1 showed a half-life similar to antibodies in the DART format (39), which is a favorable pharmacodynamic feature for cancer therapeutics (40).

The target recognized by the scDb-hERG1-β1, the hERG1/β1 complex, is a completely innovative and specific tumor antigen, expressed exclusively in cancer tissues (14). hERG1 is physiologically expressed on the plasma membrane of cardiac myocytes, where it functions as a conductive ion channel. However, when overexpressed in cancer tissues hERG1 forms a complex with β1 which operates as a signaling device, triggering Akt-centered intracellular pathways (14,19,20). The diabody format is conceived to bind to two proteins, hERG1 and β1 in our case, only when they are very close and tightly linked, as occurs in the hERG1/β1 complex (14). Indeed, ELISA assays showed a very low affinity to the single antigenic peptides, which dramatically increased when the two peptides were mixed. Cell-ELISA and IF experiments supported the specificity of the scDb-hERG1-β1 towards the hERG1/β1 complex. Consistently, the scDb-hERG1-β1 did not bind to hERG1 channels expressed in human cardiac myocytes or pancreatic beta cells (Figure 2). This lack of binding would avoid the cardiac side effects that many hERG1 blockers exert (15). Furthermore, the targeting of the complex instead of the single proteins is expected to give better performances for a cancer specific therapeutic strategy. In fact, even the targeting of β1 integrins in cancer, although repeatedly attempted, has failed to give the results obtained targeting αIIbβ3 integrins for the treatment of thrombosis or β2 integrins for treating inflammation (41), due to the high and wide expression of these integrins in normal tissues (41). Finally, the functional effects of the scDb-hERG1-β1 can be traced back to the modulation of its target, i.e. the hERG1/β1 complex, and its downstream signaling pathway centered on Akt. We previously demonstrated that the

hERG1/β1 complex interferes with p53 in CC cells (13, 19). Hence, it is not surprising that the targeting of the complex with the scDb-hERG1-β1 induces apoptosis in CC cells. In PDAC cells, where hERG1 activates EGFR signaling and hence the phosphorylation of ERK1/2 (29), it was expected that the harnessing of the hERG1/β1 complex would hesitate in a modulation of cell cycle, as indeed we showed in the present paper.

Overall, we have here provided the proof of concept of the therapeutic valence of a novel scDb-hERG1-β1, which harnesses the hERG1/β1 integrin complex in solid cancers which over express the complex. Such therapeutic antibody can be proposed either as the backbone for the development of ADCs, or in combination therapy with classical chemotherapeutic drugs.

**Conflict of interest**: C.D., S.C., L.C. and A.A. are named inventors on a patent covering the scDb-hERG1-β1 antibody and derivatives thereof. A.A. is co-founder of MCK Therapeutics Srl, spin off of the University of Florence, that owns the license of the patent. All other authors declare no potential conflicts of interests.

**Acknowledgements**

This project was supported by AIRC, Grant N° IG 15627 and IG 21510 to AA , PRIN Italian Ministry of University and Research (MIUR) "Leveraging basic knowledge of ion channel network in cancer for innovative therapeutic strategies (LIONESS)" 20174TB8KW to AA, pHioniC: European Union's Horizon 2020 grant No 813834 to AA , pHioniC Marie Curie fellowship to RB and AIRC Fellowship to Italy 2019 “Francesco Tonni”, grant 24020 to CD.

We would like to thank Prof. Andrea Becchetti for continuous helpful suggestions and for reading the manuscript.

We would like to thank Paola Defilippi and Emilia Turco (University of Turin) for kindly providing TS2/16 mAb hybridoma pellets, and SY5Y cells, Prof Mustafa Djamgoz (Imperial College, London) for kindly providing MDA-231 cells. We also thank Dr Leonardo Gonnelli (CERM University of Florenece) for the excellent technical assistance. We would also acknowledge Prof Carlo Di Mario (Cardiology Unit, AUOC, Azienda Ospedaliero Universitaria Careggi, Firenze), Dr Massimo Maccherini (Department of Cardiac Surgery of Azienda Ospedaliero Universitaria Senese) for providing cardiac tissue samples. We also would like to thank Eugenio Torre for the help in processing human primary samples and Dr Alberto Montalbano for the help in acquiring confocal microscopy images.

**Author Contributions**

**C Duranti**: investigation, formal analysis, methodology, visualisation, writing original draft, supervision. **J. Iorio**: investigation, formal analysis, writing original draft, supervision. **T. Lottini**: investigation, formal analysis, methodology. **E. Lastraioli**: formal analysis, visualisation, methodology. **S. Crescioli**: methodology, investigation. **G. Bagni**: investigation, visualisation.

**M.Lulli**: investigation. **R. Bouazzi**: investigation. **C. Capitani**: investigation. **L. Carraresi**: investigation. **M. Stefanini**: investigation. **H. De Jonge**: revision, formal analysis. **L. Iamele**: revision, formal analysis. **A. Arcangeli**: investigation, formal analysis, methodology, visualisation, writing original draft, supervision, resources, project administration, funding acquisition.

**REFERENCES**


1. Brekke OH, Sandlie I. Therapeutic antibodies for human diseases at the dawn of the twenty-first century. Nat Rev Drug Discov. 2003 Jan;2(1):52-62.
2. Shepard HM, Phillips GL, D Thanos C, Feldmann M. Developments in therapy with monoclonal antibodies and related proteins. Clin Med (Lond). **2017** Jun;17(3):220-232.
3. Thakur A, Huang M, Lum LG. Bispecific antibody based therapeutics: Strengths and challenges. Blood Rev. **2018** Jul;32(4):339-347.
4. Husain B, Ellerman D. Expanding the Boundaries of Biotherapeutics with Bispecific Antibodies. BioDrugs. **2018** Oct;32(5):441-464.
5. Krishnamurthy A, Jimeno A. Bispecific antibodies for cancer therapy: A review. *Pharmacol Ther* **1991**;185:122-34
6. Beck, A., Wurch, T., Bailly, C. & Corvaia, N. Strategies and challenges for the next generation of therapeutic antibodies. *Nature Reviews Immunology* **2010**;10:345–52.
7. Elgundi Z, Reslan M, Cruz E, Sifniotis V, Kayser V. The state-of-play and future of antibody therapeutics. *Adv Drug Deliv* Rev **2017**;122:2-19.
8. Kaplon H, Muralidharan M, Schneider Z, Reichert JM. Antibodies to watch in 2020. *MAbs* **2020**;12:1703531.
9. Birrer MJ, Moore KN, Betella I, Bates RC. Antibody-Drug Conjugate-Based Therapeutics: State of the Science. *J Natl Cancer Inst* **2019**;111:538-49.
10. Ahmad ZA, Yeap SK, Ali AM, Ho WY, Alitheen NB, Hamid M. scFv antibody: principles and clinical application. *Clin Dev Immunol* **2012**;2012:980250.
11. Huang S, van Duijnhoven SMJ, Sijts AJAM, van Elsas A. Bispecific antibodies targeting dual tumor-associated antigens in cancer therapy. *J Cancer Res Clin Oncol* **2020**. doi: 10.1007/s00432-020-03404-6.

12. Cherubini A, Hofmann G, Pillozzi S, Guasti L, Crociani O, Cilia E *et al*. Human ether-a-go-go-related gene 1 channels are physically linked to beta1 integrins and modulate adhesion-dependent signaling. *Mol Biol Cell* **2005**;16:2972-83.
13. Crociani O, Zanieri F, Pillozzi S, Lastraioli E, Stefanini M, Fiore A *et al*. hERG1 channels modulate integrin signaling to trigger angiogenesis and tumor progression in colorectal cancer. *Sci Rep* **2013**;3:3308.
14. Becchetti A, Crescioli S, Zanieri F, Petroni G, Mercatelli R, Coppola S *et al*. The conformational state of hERG1 channels determines integrin association, downstream signaling, and cancer progression. *Sci Signal* **2017**;10:eaaf3236.
15. Sanguinetti MC. HERG1 channelopathies. *Pflugers Arch* **2010**;460:265-76.
16. Mitcheson JS & Arcangeli A. The therapeutic potential of hERG1 $K^+$ channels for treating cancer and cardiac arrhythmias. In: Brian Cox and Martin Gosling, editors. Ion Channel Drug Discovery. London: Royal Society of Chemistry; 2015. p. 258-96
17. Duranti C, Arcangeli A. Ion Channel Targeting with Antibodies and Antibody Fragments for Cancer Diagnosis. *Antibodies (Basel)* **2019**;8:33.
18. Iorio J, Duranti C, Lottini T, Lastraioli E, Bagni G, Becchetti A *et al*. KV11.1 Potassium Channel and the Na+/H+ Antiporter NHE1 Modulate Adhesion-Dependent Intracellular pH in Colorectal Cancer Cells. *Front Pharmacol* **2020**;11:848.
19. Petroni G, Bagni G, Iorio J, Duranti C, Lottini T, Stefanini M *et al*. Clarithromycin inhibits autophagy in colorectal cancer by regulating the hERG1 potassium channel interaction with PI3K. *Cell Death Dis* **2020**;11:161.
20. Becchetti A, Petroni G, Arcangeli A. Ion Channel Conformations Regulate Integrin-Dependent Signaling. *Trends Cell Biol* **2019**;29:298-307.
21. Arcangeli A, Becchetti A. hERG Channels: From Antitargets to Novel Targets for Cancer Therapy. *Clin Cancer Res* **2017**;23:3-5.

22. Redfern WS, Carlsson L, Davis AS, Lynch WG, MacKenzie I, Palethorpe S *et al*. Relationships between preclinical cardiac electrophysiology, clinical QT interval prolongation and torsade de pointes for a broad range of drugs: evidence for a provisional safety margin in drug development. *Cardiovasc Res* **2003**;58:32-45.
23. Holliger P, Hudson PJ. Engineered antibody fragments and the rise of single domains. *Nat Biotechnol* 227-238**2005**;23:1126-36.
24. Kholodenko RV, Kalinovsky DV, Doronin II, Ponomarev ED, Kholodenko IV. Antibody Fragments as Potential Biopharmaceuticals for Cancer Therapy: Success and Limitations. *Curr Med Chem.* **2019**;26(3):396-426.
25. Guasti L, Crociani O, Redaelli E, Pillozzi S, Polvani S, Masselli M et al. Identification of a posttranslational mechanism for the regulation of hERG1 K+ channel expression and hERG1 current density in tumor cells. *Mol Cell Biol* **2008**;28:5043-60
26. Takada Y, Puzon W. Identification of a regulatory region of integrin beta 1 subunit using activating and inhibiting antibodies. *J Biol Chem* **1993**;268:17597-601.
27. Duranti C, Carraresi L, Sette A, Stefanini M, Lottini T, Crescioli S *et al*. Generation and characterization of novel recombinant anti-hERG1 scFv antibodies for cancer molecular imaging. *Oncotarget* **2018**;9:34972-89.
28. Sette A, Spadavecchia J, Landoulsi J, Casale S, Haye B, Crociani O *et al*. Development of novel anti-Kv 11.1 antibody-conjugated PEG-TiO2 nanoparticles for targeting pancreatic ductal adenocarcinoma cells. *J Nanopart Res* **2013**;15:2111.
29. Lastraioli E, Perrone G, Sette A, Fiore A, Crociani O, Manoli S *et al*. hERG1 channels drive tumour malignancy and may serve as prognostic factor in pancreatic ductal adenocarcinoma. *Br J Cancer* **2015**;112:1076-87.
30. Manoli S, Coppola S, Duranti C, Lulli M, Magni L, Kuppalu N *et al*. The Activity of Kv 11.1 Potassium Channel Modulates F-Actin Organization During Cell Migration of Pancreatic Ductal Adenocarcinoma Cells. *Cancers (Basel)* **2019**;11:135.

31. Lastraioli E, Iorio J, Arcangeli A. Ion channel expression as promising cancer biomarker. Biochim Biophys Acta. 2015;1848(10 Pt B):2685-702..

32. Rosati B, Marchetti P, Crociani O, Lecchi M, Lupi R, Arcangeli A *et al*. Glucose- and arginine-induced insulin secretion by human pancreatic beta-cells: the role of HERG K(+) channels in firing and release. *FASEB J* **2000**;14:2601-10.

33. Xiong C, Mao Y, Wu T, Kang N, Zhao M, Di R, Li X, Ji X, Liu Y. Optimized Expression and Characterization of a Novel Fully Human Bispecific Single-Chain Diabody Targeting Vascular Endothelial Growth Factor165 and Programmed Death-1 in Pichia pastoris and Evaluation of Antitumor Activity In Vivo. *Int J Mol Sci*. **2018** Sep 25;19(10):2900.

34. Lottini T, Stefanini S, Gargiulo S, Gramanzini M, Giustetto P, Fuchs D *et al*. Micro-ultrasound, non-linear contrast mode with microbubbles and Optical Flow software tool: together for a new translational method in the study of the tumoral rheology microenvironment. *WMIC 2017: Imaging the future from molecules to medicine* **2017**;2005001.

35. Barat B, Sirk SJ, McCabe KE, et al. Cys-diabody quantum dot conjugates (immunoQdots) for cancer marker detection. Bioconjug Chem. 2009;20(8):1474-1481.

36. Lee YJ, Jeong KJ. Challenges to production of antibodies in bacteria and yeast. J Biosci Bioeng. **2015** Nov;120(5):483-90

37. Nessler I, Khera E, Vance S, Kopp A, Qiu Q, Keating TA, Abu-Yousif AO, Sandal T, Legg J, Thompson L, Goodwin N, Thurber GM. Increased Tumor Penetration of Single-Domain Antibody-Drug Conjugates Improves In Vivo Efficacy in Prostate Cancer Models. Cancer Res. 2020;80(6):1268-1278.

38. Kontermann RE. Strategies to extend plasma half-lives of recombinant antibodies. *BioDrugs* **2009**;23:93-109.

39. Wang Q, Chen Y, Park J, Liu X, Hu Y, Wang *T et al*. Design and Production of Bispecific Antibodies. *Antibodies (Basel)* **2019**;8:43.

40. Chen, Y., Xu, Y. Pharmacokinetics of Bispecific Antibody. *Curr Pharmacol Rep* **2017**, 3, 126–137.

41. Cooper J, Giancotti FG. Integrin Signaling in Cancer: Mechanotransduction, Stemness, Epithelial Plasticity, and Therapeutic Resistance. *Cancer Cell.* **2019**;35(3):347-367.

## FIGURE LEGENDS

**Figure 1. Biochemical characterization of scDb-hERG1-β1. (A)** Schematic representation of the structure of the scDb hERG1−β1. **(B)** Amino-acid sequence of the scDb hERG1-β1. Letters are highlighted using the same color-code as in panel A **(C)** Affinity Chromatography of the supernatant obtained from 3G9 yeast colony. **(D)** SDS-PAGE and Coomassie Brilliant blue staining of the supernatants obtained from 3G5 and 3G9 yeast colonies. Different concentrations of BSA are shown in the indicated lanes. **(E)** WB of the supernatants obtained from 3G5 and 3G9 yeast colonies. The lanes "ST" in D and E indicate the molecular weight standard. The arrows in D and E indicate the molecular weight (~ 68 kDa, i.e. the molecular weight (67.74 kDa) expected by in silico analysis through the ExPASy ProtParam tool) of the scDb. **(F)** Peptide ELISA using a 1:1 mix of hERG1 S5-P peptide (hERG1) and TS2/16 peptide (β1 integrin) as coating antigen, and different concentrations of scDb-hERG1-β1. **(G)** Peptide ELISA assay performed using the S5-Pore peptide (hERG1) and the β1 peptide (β1 integrin) as coating antigens and testing different concentrations of scDb-hERG1-β1. **(H)** Cell ELISA on cell lines with different expression of the hERG1/β1 complex (see text), using different concentrations (5-40 μg/ml) of scDb-hERG1-β1. Values in F, G and H are expressed as $OD_{450}$ and are means ± SEM of three independent experiments. *, $P < 0.05$; **, $P < 0.01$ and ***, $P < 0.001$.

**Figure 2. Immunofluorescence (IF) and immunohistochemistry (IHC) of scDb-hERG1-β1 on cells and tissues. (A)** Indirect IF on cells with different amounts of the hERG1/β1 complex (see text). **(B)** Indirect IF and **(C)** IHC on normal human atrial tissues using the scDb-hERG1-β1, the scFv-hERG1 and the mAb hERG1 at the indicated concentrations. Scale bar: 100 μm. **(D)** IHC on different cancer and normal tissues using the scDb-hERG1-β1 at 20 μg/ml. Scale bar: 200 μm. In the panel indicated as "NORMAL PANCREAS" a pancreatic insula labelled with the scDb is shown; in the inset a magnified (Scale bar :400 μm) insula, labeled with the mAb hERG1 is reported. The arrow indicates hERG1-positive putative insulin secreting cells.

**Figure 3. Effects of the scDb-hERG1-β1 on hERG1/β1 complex, intracellular signaling, cell viability and proliferation. (A)** co-IP of hERG1 and β1 integrin, and WB of pAKT and HIF-1α in HCT116 cells cultured over night in complete medium in the absence (CTR= Control untreated cells) or in the presence of scDb-hERG1-β1 (scDb) at 100 μg/ml. Densitometric analyses, calculated as in (14), relative to three independent experiments are shown in the histograms on the right. ***, $P < 0.001$. **(B)** co-IP of hERG1 and β1 integrin, and WB of pAKT and HIF-1α in PANC-1 treated as in (A). Densitometric analyses, calculated as in (14), relative to three independent experiments are shown in the histograms on the right. ***, $P < 0.001$. **(C)** $IC_{50}$ values of the scDb-hERG1-β1 on cell vitality in different cell lines. **(D)** Cell vitality of HCT116 and PANC-1 cells treated with the scDb-hERG1-β1, the mAb hERG1 or the mAb β1TS2/16 at the concentrations indicated in the figure. **(E)** HCT116 growth rate using the scDb-hERG1-β1 at the $IC_{50}$ dose. Values in panels (D) and (E) are means ± SEM of three independent experiments. *, $P < 0.05$; **, $P < 0.01$ and ***, $P < 0.001$. **(G)** PANC-1 growth rate using the scDb-hERG1-β1 at the $IC_{50}$ dose. Values in panels (D) and (E) are means ± SEM of three independent experiments. *, $P < 0.05$; **, $P < 0.01$ and ***, $P < 0.001$. **(F)** Representative Dot Plots of Annexin/PI test and cell cycle on HCT116 cells, untreated (CTR= Control) or treated with scDb-hERG1-β1 (scDb) at the $IC_{50}$ dose. Representative of three different experiments. **(H)** Representative Dot Plots of

Annexin/PI test and cell cycle of PANC-1 cells, untreated (CTR= Control) or treated with scDb-hERG1-β1 (scDb) at the $IC_{50}$ dose. Representative of three different experiments.

**Figure 4. Effects of the scDb-hERG1-β1 on 3D growth and cell motility. (A)** Growth curves of spheroids obtained from HCT116, PANC-1 and HEK 293 cells treated with the scDb-hERG1-β1 at their respective $IC_{50}$ values. **(B)** Growth curves of spheroids obtained from HCT 116, treated with mAb hERG1 or mAb β1TS2/16 at 100 μg/ml. (**C**) Growth curves of spheroids obtained from HCT 116 and PANC-1 cells, treated with scDb-hERG1-β1 as indicated. Motility Index (MI) of different cell lines treated for 24 hours with (**D**) the scDb-hERG1-β1 at their respective $IC_{50}$ dose; **(E)** the scDb-hERG1-β1 at 50 μg/ml ; **(F)** mAb hERG1 or mAb β1TS2/16 at 100 μg/ml. All the values are expressed as means ± SEM of three independent experiments. *, $P < 0.05$; **, $P < 0.01$ and ***, $P < 0.001$.

**Figure 5. Pharmacokinetic and toxicity *in vivo* of the scDb-hERG1-β1. (A)** Serum stability of the scDb-hERG1-β1 (20 μg/ml) in mouse serum at 37°C. **(B)** *In vivo* half-life of scDb-hERG1-β1 injected i.v. at 8 mg/Kg in nu/nu mice. In A and B values are expressed as $OD_{450}$ and are means **±** SEM of three independent experiments. The half-life (T ½) is calculated as detailed in Supplementary methods. **(C)** IHC staining with anti-6xHis antibodies of heart, kidney and liver of mice treated with either vehicle (CTR, upper panels) or 8 mg/Kg scDb (scDb, lower panels). Scale bar: 200 μm. **(D)** ECG of mice treated as in (C) **(E)** Perfusion index (PI) measured on kidneys of mice treated as in (C), after different times of treatment. **(F)** H&E staining on kidneys of mice treated as in (C) for 24 hours. Scale bar: 100 μm. Insets show a higher magnification of the renal areas where no signs of toxicity are evident.

**Figure 6. *In vivo* effects of the scDb-hERG1-β1 on CC or PDAC xenografted tumor masses. (A),** (**B**) -Schedule of treatment. IHC staining with anti-6x_His antibodies of tumor masses obtained by s.c. injection of CC HCT116-cells treated with the scDb-hERG1-β1 (scDb) or with the vehicle

(CTR= Control). Scale bar: 200 μm. The bar graphs on the right show the densitometric analyses and significance. * p<0.05; ** p< 0.01; ***p< 0.001. **(C)** Time course of the volume of s.c. xenografts of –CC HCT116 cells, treated as in (A) **(D)** Representative high-resolution ultrasound images of tumor masses derived from injection of HCT116 cells with the corresponding OxyHemo photoacoustic images; red areas indicate well oxygenated parts whereas blue and dark areas indicate the presence of hypoxia; **(E)** IHC staining with anti-pAkt and anti-HIF-1α antibodies of tumor masses obtained by s.c. injection of HCT116. **(F), (G)** Schedule of treatment. IHC staining with anti-6x_His antibodies of tumor masses obtained by s.c. injection of PDAC PANC-1 cells treated with the scDb-hERG1-β1 (scDb) or with the vehicle (CTR= Control). Scale bar: 200 μm. The bar graphs on the right show the densitometric analyses and significance. * p<0.05; ** p< 0.01; ***p< 0.001. **(H)** Time course of the volume of s.c. xenografts of PDAC PANC-1 cells, treated as in (F). **(I)** Representative ultrasound images of tumor masses from PANC-1 cells at day 33. In D and I the 3D tumor reconstruction obtained through by Vevo Lab software are reported in the adjacent panels. (**J**) IHC staining with anti-pAkt and anti-HIF-1α antibodies of tumor masses obtained by s.c. injection of–PANC-1 cells. Scale bar: 200 μm. The bar graphs on the right show the densitometric analyses and significance. * p<0.05; ** p< 0.01; ***p< 0.001.

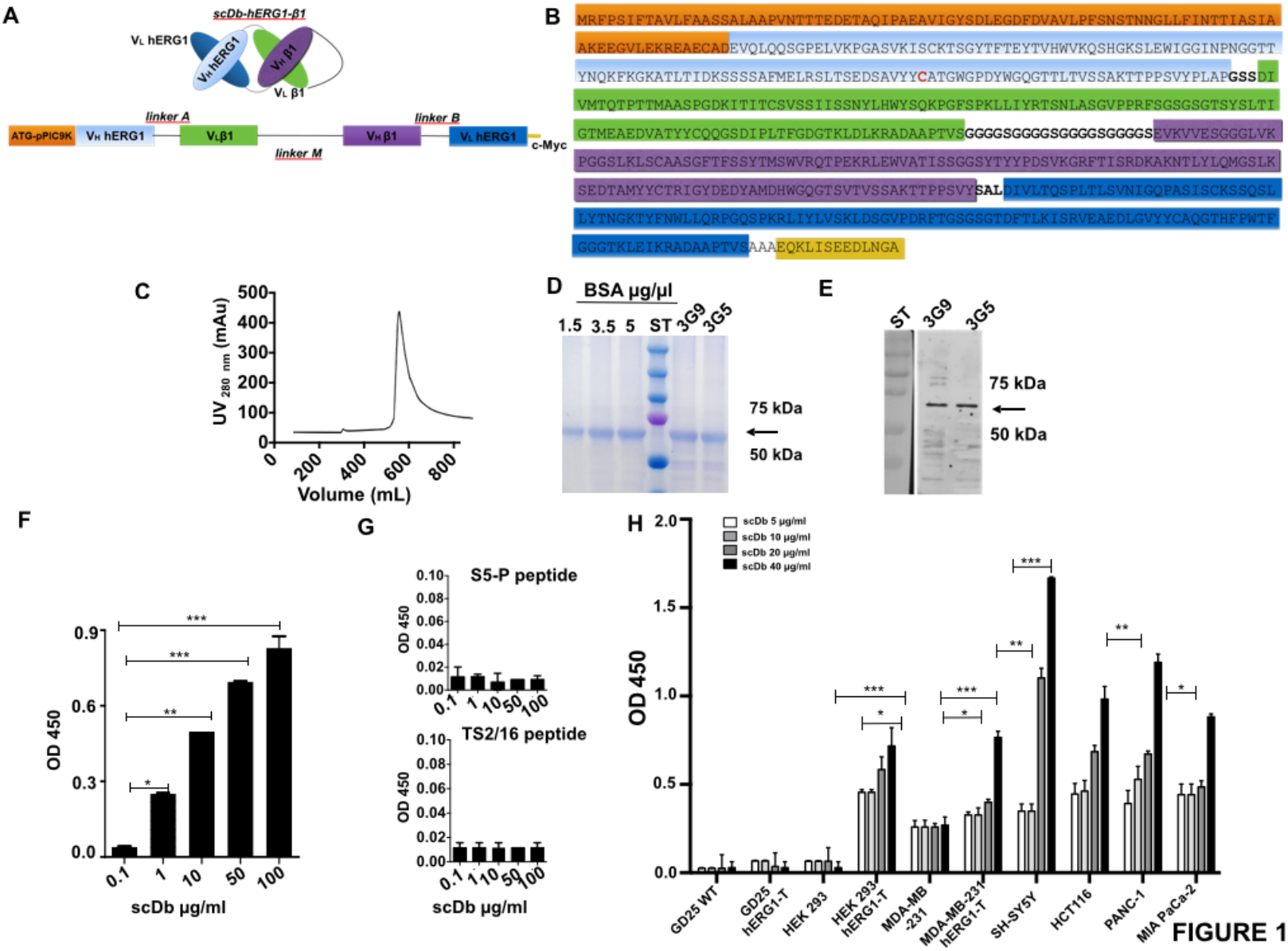
A
scDb-hERG1-β1
VL hERG1
VH hERG1
VH β1
VL β1
linker A
linker B
linker M
ATG-pPIC9K
VH hERG1
VLβ1
VH β1
VL hERG1
c-Myc
B
MRFPSIFTAVLFAASSALAAPVNTTTEDETAQIPAEAVIGYSDLEGDFDVAVLPFSNSTNNGLLFINTTIASIA
AKEEGVLEKREAECADEVQLQQSGPELVKPGASVKISCKTSGYTFTEYTVHWVKQSHGKSLEWIGGINPNGGTT
YNQKFKGKATLTIDKSSSSAFMELRSLTSEDSAVYYCATGWGPDYWGQGTTLTVSSAKTTPPSVYPLAPGSSDI
VMTQTPTTMAASPGDKITITCSVSSIISSNYLHWYSQKPGFSPKLLIYRTSNLASGVPPRFSGSGSGTSYSLTI
GTMEAEDVATYYCQQGSDIPLTFGDGTKLDLKRADAAPTVSGGGGSGGGGSGGGGSGGGGSEVKVVESGGGLVK
PGGSLKLSCAASGFTFSSYTMSWVRQTPEKRLEWVATISSGGSYTYYPDSVKGRFTISRDKAKNTLYLQMGSLK
SEDTAMYYCTRIGYDEDYAMDHWGQGTSVTVSSAKTTPPSVYSALDIVLTQSPLTLSVNIGQPASISCKSSQSL
LYTNGKTYFNWLLQRPGQSPKRLIYLVSKLDSGVPDRFTGSGSGTDFTLKISRVEAEDLGVYYCAQGTHFPWTF
GGGTKLEIKRADAAPTVSAAAEQKLISEEDLNGA
C
UV 280 nm (mAu)
Volume (mL)
D
BSA μg/μl
1.5 3.5 5 ST 3G9 3G5
75 kDa
50 kDa
E
ST 3G9 3G5
75 kDa
50 kDa
F
OD 450
scDb μg/ml
G
S5-P peptide
TS2/16 peptide
OD 450
scDb μg/ml
H
scDb 5 μg/ml
scDb 10 μg/ml
scDb 20 μg/ml
scDb 40 μg/ml
OD 450
GD25 WT
GD25 hERG1-T
HEK 293
HEK 293 hERG1-T
MDA-MB -231
MDA-MB-231 hERG1-T
SH-SY5Y
HCT116
PANC-1
MIA PaCa-2

FIGURE 1

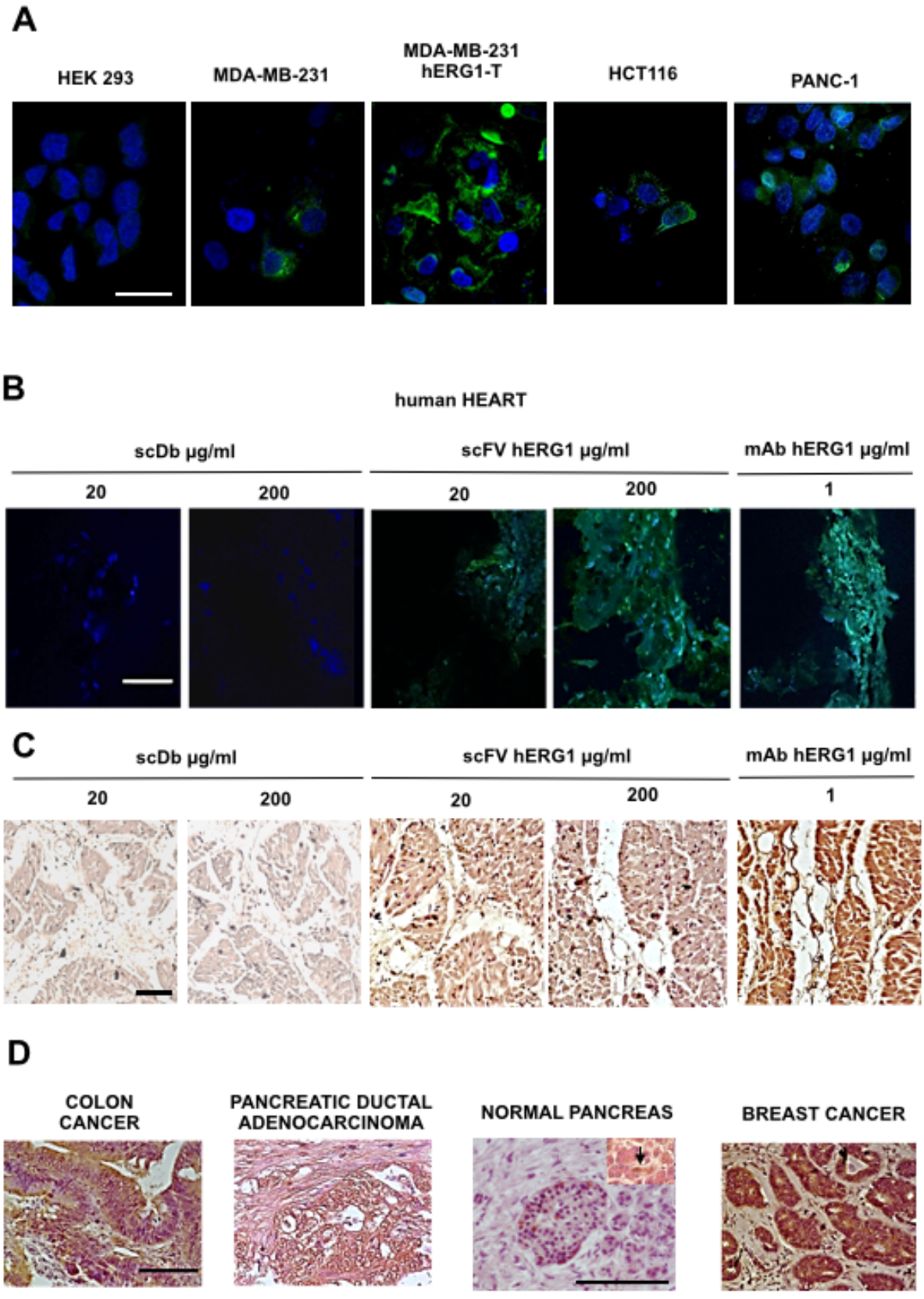
A
HEK 293
MDA-MB-231
MDA-MB-231 hERG1-T
HCT116
PANC-1
B
human HEART
scDb µg/ml
20
200
scFV hERG1 µg/ml
20
200
mAb hERG1 µg/ml
1
C
scDb µg/ml
20
200
scFV hERG1 µg/ml
20
200
mAb hERG1 µg/ml
1
D
COLON CANCER
PANCREATIC DUCTAL ADENOCARCINOMA
NORMAL PANCREAS
BREAST CANCER

FIGURE 2

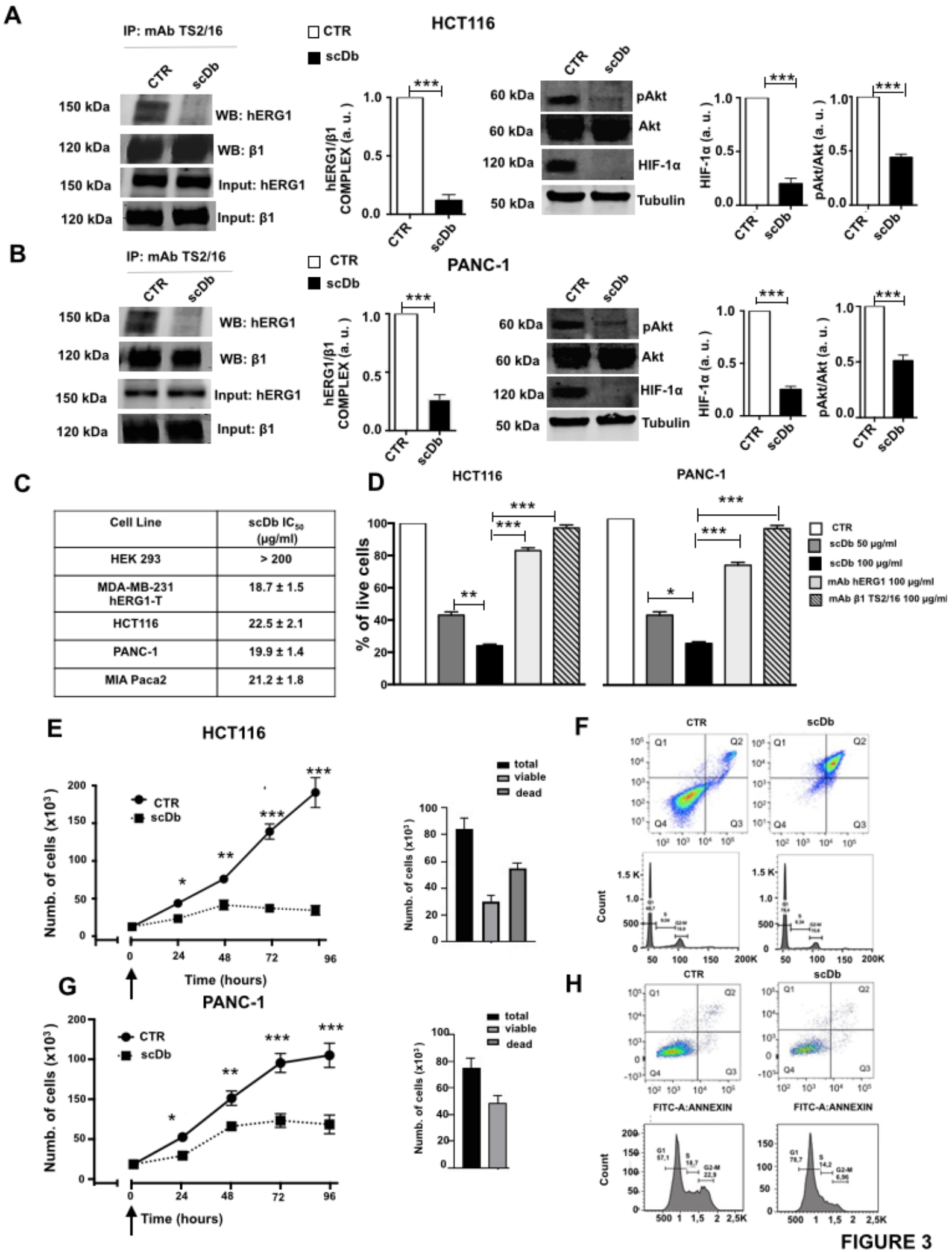


| Cell Line | scDb $IC_{50}$ (µg/ml) |
|---|---|
| HEK 293 | > 200 |
| MDA-MB-231 hERG1-T | 18.7 ± 1.5 |
| HCT116 | 22.5 ± 2.1 |
| PANC-1 | 19.9 ± 1.4 |
| MIA Paca2 | 21.2 ± 1.8 |

FIGURE 3

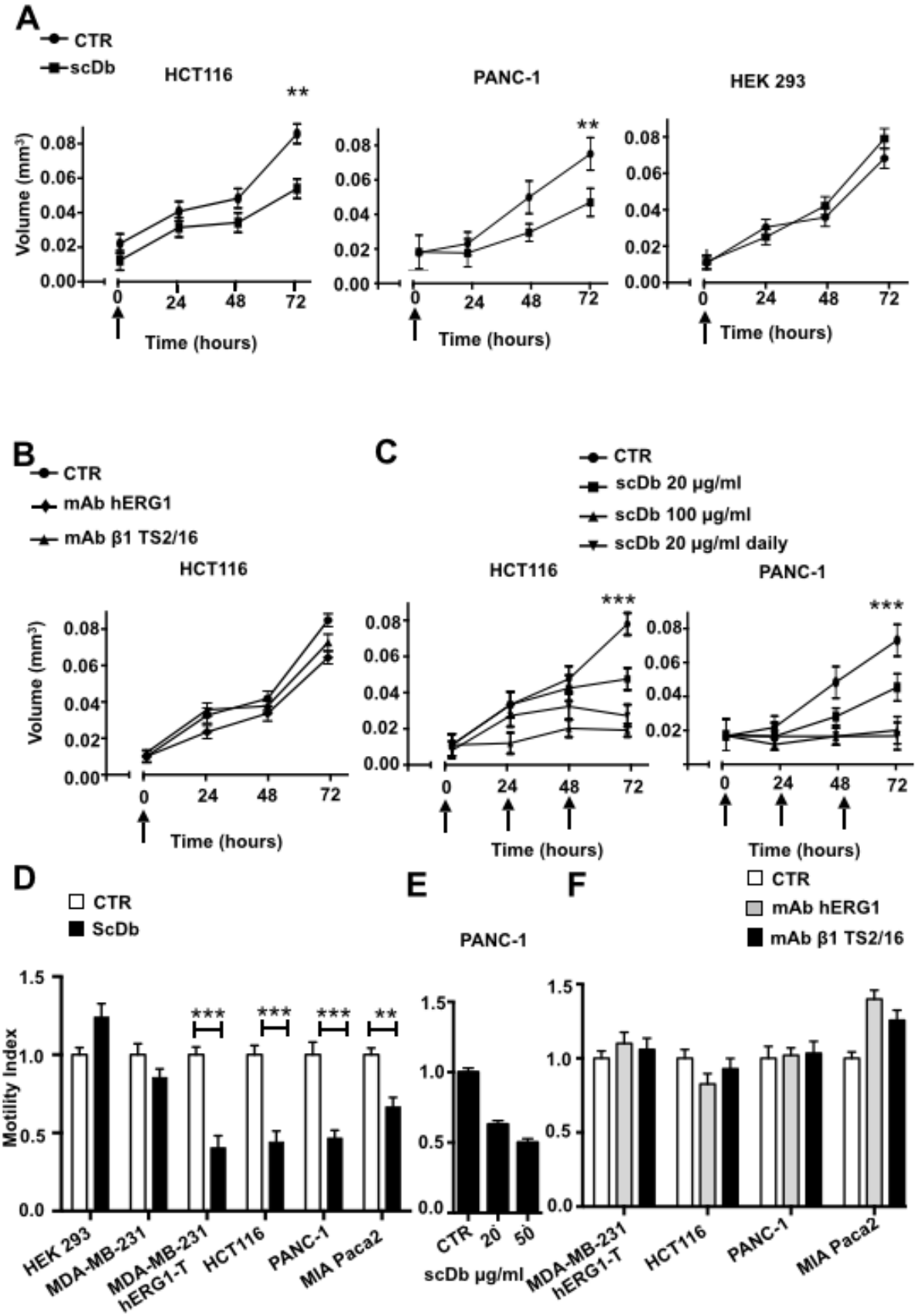
A
CTR
scDb
HCT116
PANC-1
HEK 293
Volume (mm³)
Time (hours)
B
CTR
mAb hERG1
mAb β1 TS2/16
HCT116
C
CTR
scDb 20 µg/ml
scDb 100 µg/ml
scDb 20 µg/ml daily
HCT116
PANC-1
D
CTR
ScDb
Motility Index
HEK 293
MDA-MB-231
MDA-MB-231 hERG1-T
HCT116
PANC-1
MIA Paca2
E
PANC-1
CTR
20
50
scDb µg/ml
F
CTR
mAb hERG1
mAb β1 TS2/16
MDA-MB-231 hERG1-T
HCT116
PANC-1
MIA Paca2

FIGURE 4

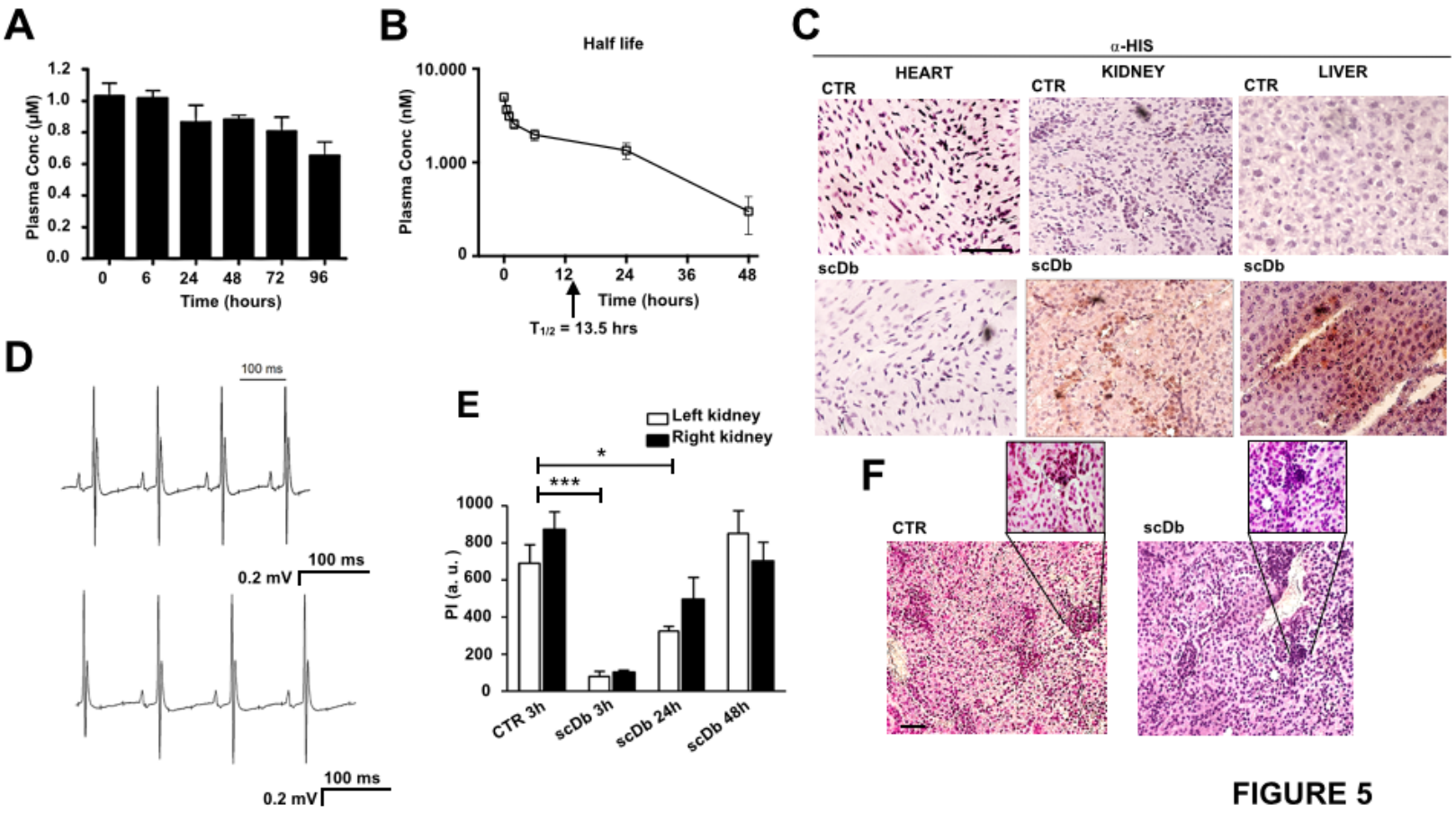
A
Plasma Conc (μM)
1.2
1.0
0.8
0.6
0.4
0.2
0.0
0
6
24
48
72
96
Time (hours)
B
Half life
Plasma Conc (nM)
10.000
1.000
0
0
12
24
36
48
Time (hours)
T1/2 = 13.5 hrs
C
α-HIS
HEART
KIDNEY
LIVER
CTR
CTR
CTR
scDb
scDb
scDb
D
100 ms
100 ms
0.2 mV
100 ms
0.2 mV
E
Left kidney
Right kidney
*
***
PI (a. u. )
1000
800
600
400
200
0
CTR 3h
scDb 3h
scDb 24h
scDb 48h
F
CTR
scDb

FIGURE 5

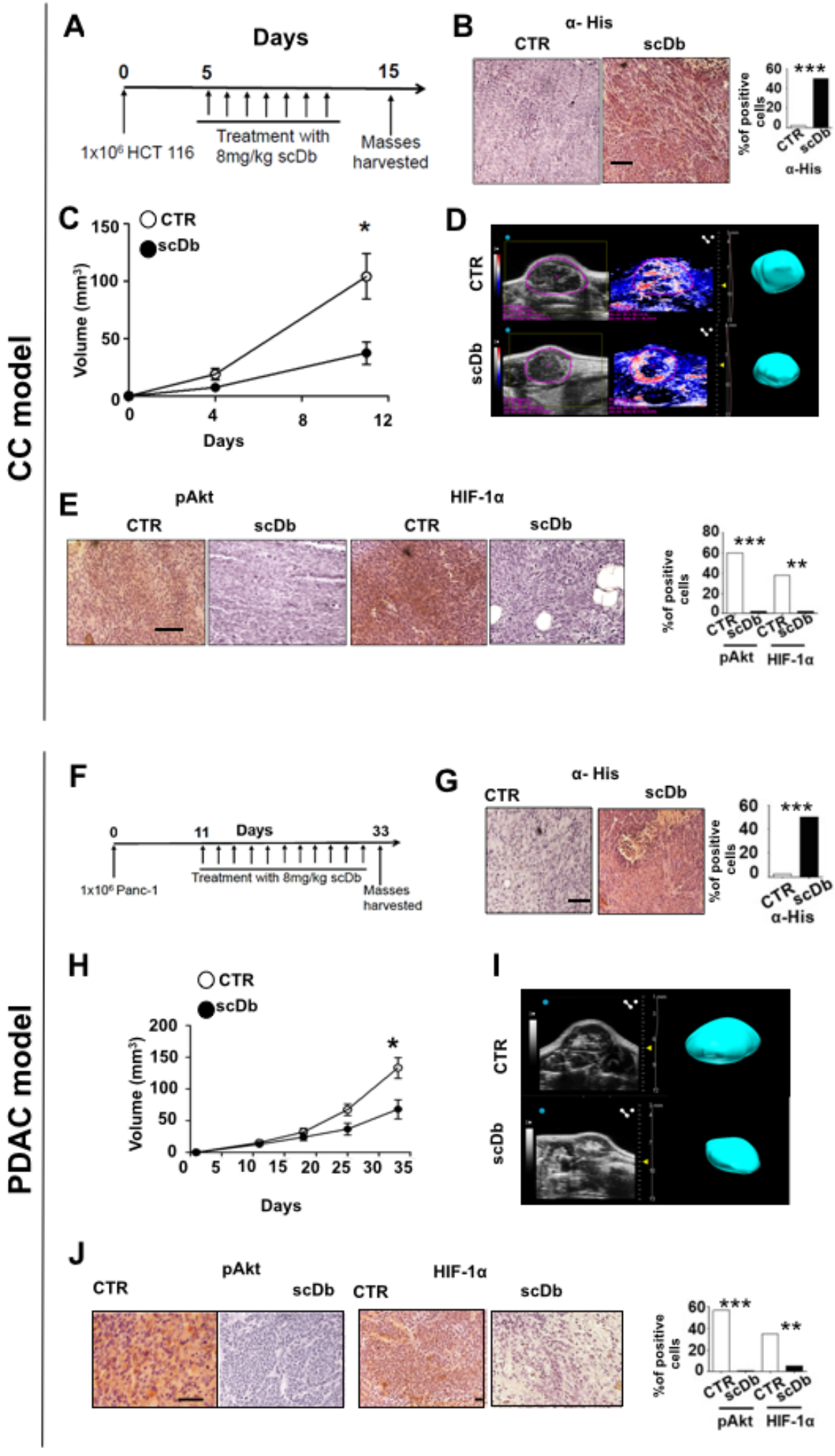
CC model
A
Days
0
5
15
1x10⁶ HCT 116
Treatment with 8mg/kg scDb
Masses harvested
B
α- His
CTR
scDb
%of positive cells
***
CTR
scDb
α-His
C
CTR
scDb
Volume (mm³)
*
Days
D
CTR
scDb
E
pAkt
HIF-1α
CTR
scDb
CTR
scDb
%of positive cells
***
**
pAkt
HIF-1α
PDAC model
F
0
11
Days
33
1x10⁶ Panc-1
Treatment with 8mg/kg scDb
Masses harvested
G
α- His
CTR
scDb
%of positive cells
***
α-His
H
CTR
scDb
Volume (mm³)
*
Days
I
CTR
scDb
J
pAkt
HIF-1α
CTR
scDb
CTR
scDb
%of positive cells
***
**
pAkt
HIF-1α

FIGURE 6

# scDb-hERG1-β1

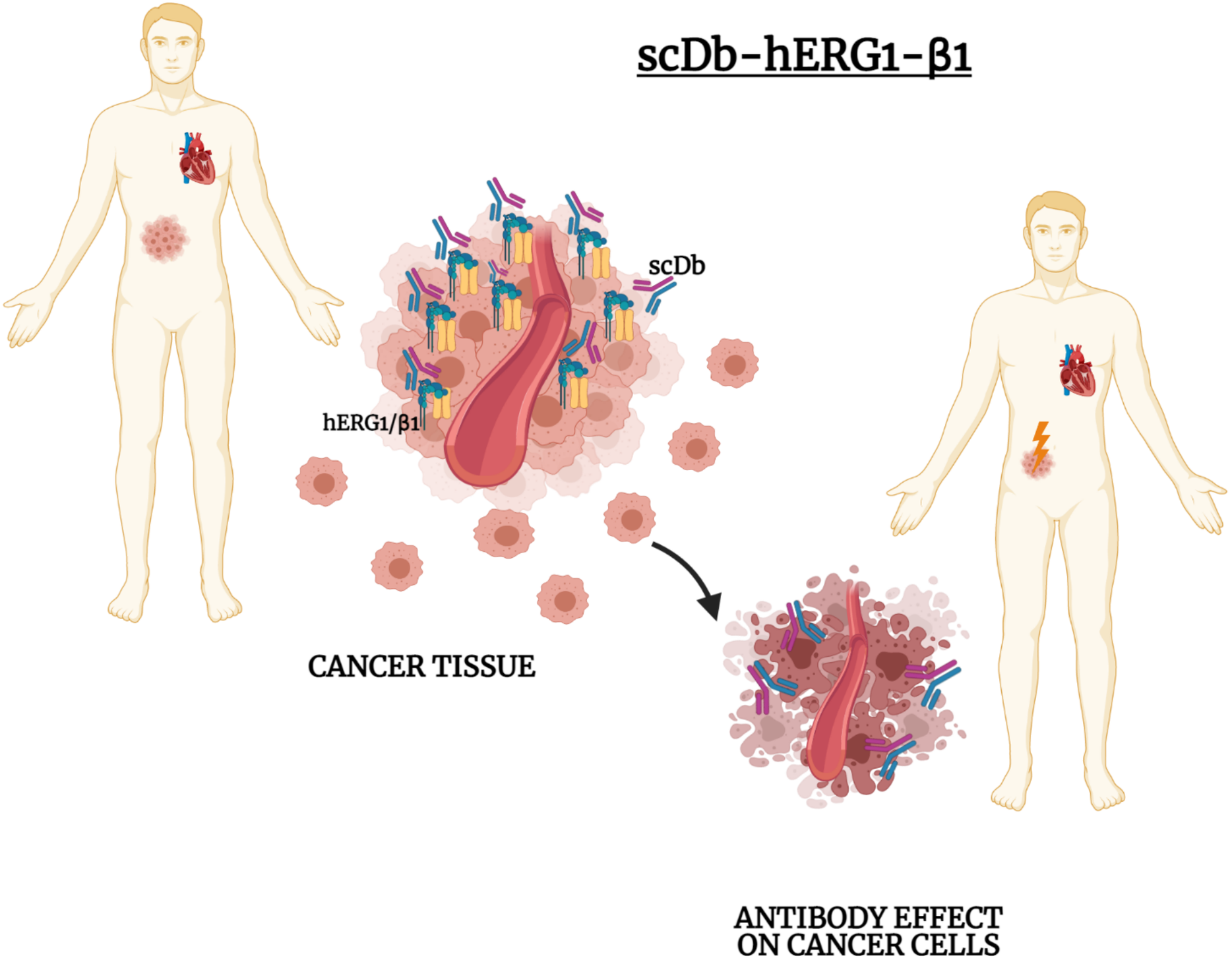


scDb-hERG1-β1 antibody targets hERG1/β1 complex on tumor cells, impairing tumor growth, without effects on the heart